

Intermediate Scaling and Logarithmic Invariance in Turbulent Pipe Flow

Sourabh S. Diwan* and Jonathan F. Morrison†

Department of Aeronautics, Imperial College London, South Kensington, London SW7 2AZ.

(Dated: September 27, 2019)

A three-layer asymptotic structure for turbulent pipe flow is proposed, revealing in terms of intermediate variables, the existence of a Reynolds-number invariant logarithmic region. It provides a theoretical foundation for addressing important questions in the scaling of the streamwise mean velocity and variance. The key insight emerging from the analysis is that the scale separation between two adjacent layers is proportional to $\sqrt{Re_\tau}$, rather than Re_τ . This suggests that, in order to realise Reynolds-number asymptotic invariance, much higher Reynolds numbers may be necessary to achieve sufficient scale separation. The formulation provides a theoretical basis for explaining the presence of a power law for the mean velocity in pipe flow at low Reynolds numbers and the co-existence of power and log laws at higher Reynolds numbers. Furthermore, the Townsend-Perry ‘constant’ for the variance is shown to exhibit a systematic Reynolds-number dependence.

The drag coefficient of a turbulent boundary layer decreases indefinitely with increasing Reynolds number because the small-scale motion near the surface is always directly affected by viscosity. Reynolds number similarity is therefore an essential tool in the scaling and modelling of near-wall flow. One of the cornerstones in the theory of turbulent wall flows is the logarithmic (“log”) variation of the mean velocity (Eq. 1) in the inertial sublayer:

$$U^+ = \frac{1}{\kappa} \ln(y^+) + A, \quad (1)$$

where $U^+ = U/u_\tau$ and $y^+ = yu_\tau/\nu$; U is the mean streamwise velocity, y is the wall-normal distance, ν is the kinematic viscosity, $u_\tau = \sqrt{\tau_w/\rho}$ is the friction velocity, τ_w is the wall shear stress and ρ is the density. κ in Eq. (1) is the well-known von Kármán constant.

Another celebrated result in wall turbulence is Townsend’s “attached-eddy” hypothesis [1], which predicts a logarithmic profile for the streamwise (and spanwise) velocity variance in the inertial sublayer. For pipe flows, the log law for streamwise variance takes the form:

$$\frac{\overline{u^2}}{u_\tau^2} = B_1 - A_1 \ln\left(\frac{y}{R}\right), \quad (2)$$

where u is fluctuating streamwise velocity, R is the pipe radius and the overbar indicates time averaging. A_1 and B_1 are proportionality constants, and A_1 is called the Townsend-Perry constant [2]. Perry and Chong [3] showed that the log law for the mean velocity (Eq. 1) and that for the streamwise variance (Eq. 2) can be derived as dual conditions using the attached-eddy formulation.

There remain some central, yet open, questions regarding the Reynolds-number invariance and universality of the von Kármán constant [1, 4–6] that have received much attention, especially for pipe flow [7–9]. By comparison, the Reynolds-number dependence of the Townsend-Perry constant has received rather less attention [10–12].

There have also been alternative formulations for the mean velocity, e.g. the power-law variation proposed by

Barenblatt [13] for pipe and channel flows. Zagarola and Smits [14] used a general matching principle involving different velocity scales for the inner and outer layers, arguing that as long as the ratio of the velocity scales is a function of Reynolds number, the mean velocity is expected to follow a power law. Princeton superpipe measurements show that, at very high Reynolds numbers, $Re_\tau = Ru_\tau/\nu = O(10^5)$, a power law is present in the lower part of the overlap region followed by the log law further away from the wall; see also [15, 16].

In this Letter, we propose a theoretical framework, in the context of the turbulent pipe flow, for addressing some of the outstanding issues outlined above. We seek Reynolds-number scaling of the mean velocity and variance in the intermediate region of the pipe flow using the length scale, $y_m^+ \propto \sqrt{Re_\tau}$ and the velocity scale (u_m) equal to the rms velocity at $y = y_m$. We propose the existence of a distinct intermediate layer (with scales y_m and u_m), in addition to the classical inner and outer layers, implying a three-layer asymptotic structure for pipe flow. It should be noted that scaling with $\sqrt{Re_\tau}$ is that of the “meso-layer”, a term that has been used in the literature with different connotations – either to indicate the location of the peak in the Reynolds shear stress [17] or to provide an offset for the log-law origin in the inertial sublayer [7] or to indicate a region where the turbulent inertia, pressure gradient and viscous forces are in balance [18]. Here therefore, we use the term “intermediate layer”, defined as a layer of finite thickness centered on $y/y_m = 1$ with scales (y_m, u_m) . This definition is closer in spirit to the intermediate layer proposed by Afzal [19].

The present analysis is based on the NSTAP data measured in the Princeton Superpipe [16]. Fig. 1 shows scaling of the streamwise variance with length scale, $y_m^+ = 3.5\sqrt{Re_\tau}$ and velocity scale, $u_m = \sqrt{\overline{u^2}}(y = y_m)$: there is an excellent collapse of the profiles in the region around $y/y_m = 1$ for two decades in Re_τ , $1,985 \leq Re_\tau \leq 98,190$; this is the motivation for using u_m as the intermediate velocity scale. The choice of constant used in the definition of y_m^+ is guided by the coefficients for $\sqrt{Re_\tau}$ used

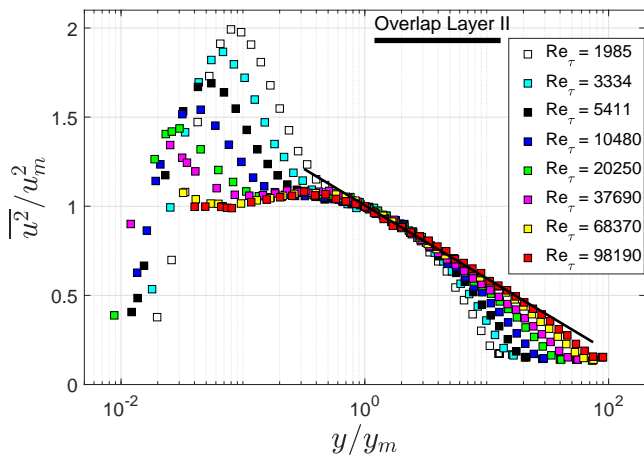


FIG. 1. Streamwise variance profiles in a smooth pipe scaled on the intermediate variables y_m and u_m ; data from Hultmark et al. [16]. The solid line is the log-law fit.

in previous definitions of the meso-layer location, e.g. $2\sqrt{Re_\tau}$ [17], or in determining the lower bound of the inertial sublayer, $3\sqrt{Re_\tau}$ [2]. Here, a slightly higher value of 3.5 is chosen to provide a better Re_τ scaling of the variance profiles for the pipe as well as boundary layer data (not shown). Note that the qualitative (and, to certain extent, quantitative) nature of the results is unaffected by the precise choice of this constant.

Taking U_m as the mean velocity at $y = y_m$, Fig. 2 shows, in defect form, the corresponding mean velocity profiles scaled on u_m . Excellent scaling is also apparent around $y/y_m = 1$. These scalings suggest the existence of a distinct, asymptotic intermediate layer lying between the classical inner and outer layers. This implies that there exists *two* asymptotic overlap regions: one between the inner and intermediate layers (“Overlap Layer I”) and the other between the intermediate and outer layers (“Overlap Layer II”) [19]. We choose the velocity scales in the inner and outer layers as u_i and u_o respectively, which are expected to be different from u_m . This is in contrast to the earlier formulations [17, 19, 20], which used the same velocity scale, u_τ , for all the layers considered. Note also that the five-layer description proposed by Vallikivi et al. [21] (based on the spectral characteristics of the streamwise velocity) is different in spirit to the present formulation which, including the two overlap layers, also proposes a total of *five* layers.

For the Overlap Layer I, the inner and intermediate scaling laws are written as,

$$U^+ = f(y^+), \quad \frac{U - U_m}{u_m} = g(\zeta), \quad (3)$$

where $\zeta = y/y_m$. Asymptotic matching of the velocity gradients for the inner and intermediate layers gives:

$$y^+ f'(y^+) = \Lambda_I \zeta g'(\zeta), \quad (4)$$

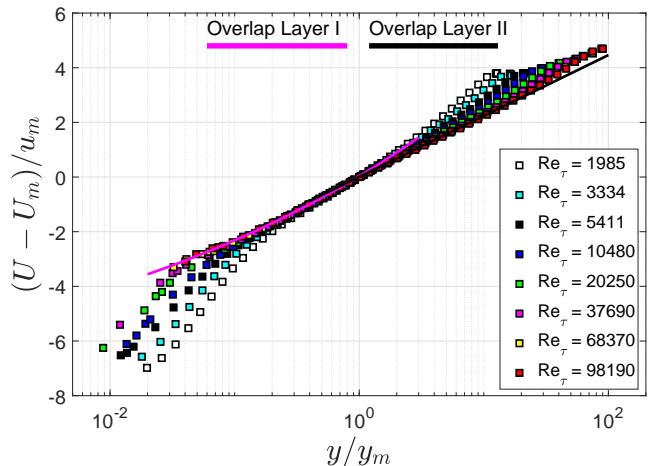


FIG. 2. Streamwise mean velocity defect scaled on the intermediate variables. The magenta line indicates a power-law fit and the black line indicates the log-law fit.

where $\Lambda_I = u_m/u_\tau$ and (\prime) indicates derivatives with respect to the corresponding independent variables. When Λ_I is Reynolds-number dependent, Eq. (4) does not imply log-law scaling. Then, Reynolds-number similarity can be achieved by simultaneously matching both velocity and velocity gradient in the overlap region [14]. This results in a power law for the mean velocity:

$$f(y^+) = U^+ = C(y^+)^{\gamma}, \quad (5)$$

$$\frac{U_m}{u_m} + g(\zeta) = \frac{U}{u_m} = C_m \left(\frac{y}{y_m} \right)^{\gamma},$$

where γ , C and C_m are constants. Alternatively, when $\Lambda_I = \text{constant}$, a log law is obtained in the overlap region.

Fig. 3(a) shows the variation of Λ_I with Reynolds number, where it continues to increase even at the highest Reynolds number. Therefore, the Overlap Layer I is governed by a power law up to $Re_\tau \approx 10^5$. Fitting a power-law curve to the U/u_m data for $0.06 \leq y/y_m \leq 0.8$, $Re_\tau = 98,190$ gives the power-law constants as $\gamma = 0.14$ and $C_m = 8.51$. Note that γ is independent of Re_τ , whereas C_m shows a weak Re_τ -dependence in a way that is consistent with $(U - U_m)/u_m$ being Reynolds-number independent. Using these parameters, the variation of $(U - U_m)/u_m$ is plotted in Fig. 2 as a magenta line which fits the data quite well in Overlap Layer I. To determine C , we separately fit a power law to the inner-scaled data (not shown here) for $Re_\tau = 98,190$ in the corresponding range, $65 \leq y^+ \leq 880$ [see 16]. This yields the same value of $\gamma = 0.14$, with $C = 8.47$. These values are close to $\gamma = 0.142$ and $C = 8.48$ reported by [15].

Overlap Layer II is bounded by the intermediate layer and the outer layer. The scaling law for the mean velocity in the outer layer can be written as

$$\frac{U_{CL} - U}{u_o} = h\left(\frac{y}{R}\right), \quad (6)$$

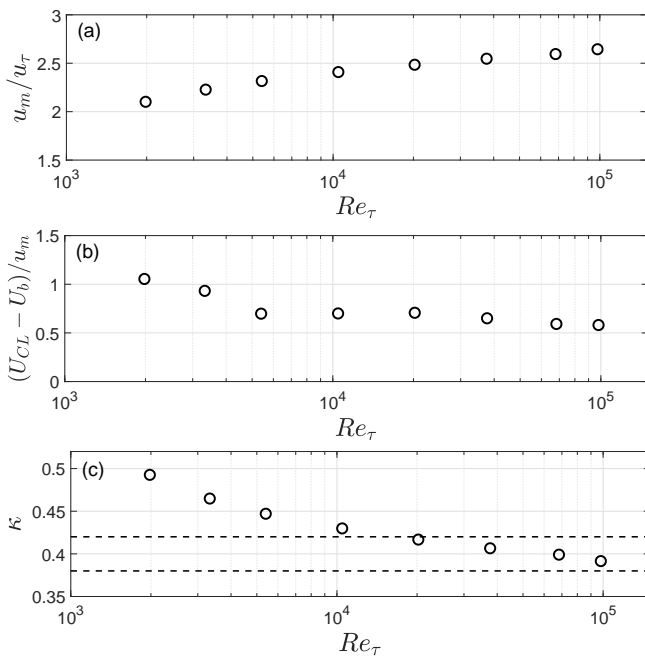


FIG. 3. Variation with Re_τ of, (a): $\Lambda_{II} = u_m/u_\tau$, (b): $\Lambda_{II} = (U_{CL} - U_b)/u_m$, (c): κ obtained from Eq. (9).

where U_{CL} is the pipe centre-line velocity. It can be seen that the character of the mean velocity in Overlap Layer II is determined by the velocity-scale ratio, $\Lambda_{II} = u_o/u_m$ (Eq. 3). Note that although Eq. (6) is written in a Reynolds-number-invariant form, the appropriate velocity scale, u_o , that would result in Reynolds-number similarity in the outer region is still unknown [22].

The two alternatives for u_o that have been used so far are u_τ and $U_{CL} - U_b$ [14], where U_b is the bulk velocity. Choosing $u_o = u_\tau$, $\Lambda_{II} = 1/\Lambda_I$, implying (Fig. 3a) that Overlap Layer II is also governed by a power law for the entire Re_τ range. This would be a surprising result as there has been overwhelming support in favour of the log law. If, on the other hand, we choose $u_o = (U_{CL} - U_b)$ we get $\Lambda_{II} = (U_{CL} - U_b)/u_m$ – see Fig. 3(b), which shows that Λ_{II} is a strong function of Re_τ for $Re_\tau \lesssim 10^4$. Assuming that Λ_{II} is approximately constant for $Re_\tau > 10^4$, the log law is recovered for the mean velocity in Overlap Layer II, which, with intermediate variables, can be written as:

$$\frac{U - U_m}{u_m} = \frac{1}{\kappa_m} \ln\left(\frac{y}{y_m}\right) + A_m. \quad (7)$$

To obtain κ_m and A_m , we fit a least-square straight line through the mean velocity data (black solid line in Fig. 2) for the two highest Reynolds numbers, $Re_\tau = 68, 370$ and $Re_\tau = 98, 190$, and for $1.2 \leq (y/y_m) \leq 13$, equivalent to $4.2\sqrt{Re_\tau} \leq y^+ \leq 0.145Re_\tau$ for $Re_\tau = 98, 190$, which is broadly consistent with the range used in [2]. The fit gives the following values for the constants:

$$\kappa_m = 1.034 \quad A_m = 0.0084. \quad (8)$$

Note that, provided the Reynolds-number similarity in the intermediate layer is ensured, the value of κ_m is independent of the choice of the coefficient in the definition of y_m . The value of A_m , however, depends on this choice (Eq. 7). The classical log-law constants can be expressed in terms of κ_m and A_m (Eqs. 1,7) as:

$$\kappa = \frac{\kappa_m}{(u_m/u_\tau)}, \quad (9)$$

$$A = \frac{u_m}{u_\tau} \left\{ \left[\frac{U_m}{u_m} + A_m \right] - \frac{1}{\kappa_m} \ln(y_m^+) \right\}.$$

κ obtained from Eq. (9) is plotted in Fig. 3(c) and shows a systematic decrease with Reynolds number; see also table 1. For $Re_\tau > 10^4$, κ falls within the uncertainty band of 0.4 ± 0.02 [9], shown as dashed lines in the figure; the trend exhibited by κ within the band can be traced back to the weak variation in Λ_{II} for $Re_\tau > 10^4$ (Fig. 3b). For $Re_\tau < 10^4$, the values of κ (and A ; table 1) are much higher than those which could be reasonably associated with the log law. This suggests that the mean velocity profile in Overlap Layer II should really follow a power law for these lower Reynolds numbers, as also implied by the strong Reynolds-number dependence of Λ_{II} for $Re_\tau < 10^4$ (Fig. 3b). Moreover, at these Reynolds numbers the two overlap layers may not be entirely distinct and therefore the two power laws may appear indistinguishable (Fig. 2). These results are consistent with the observations in [14] and [15].

The presence of a power law in Overlap Layer I and of the log law in Overlap Layer II, for $Re_\tau > 10^4$, supports the observation by Zagarola and Smits [14] [see also 16] that, at high Re_τ , the mean velocity initially follows a power-law profile followed by the log-law variation. While in these analyses the power and log laws share the same overlap region, in the present three-layer formulation they occupy two different overlap regions. This provides an explanation for the co-existence of the power and log-law profiles in the pipe flow at a given (and sufficiently large) Reynolds number. Furthermore, since the length scale for the intermediate layer is $\propto \sqrt{Re_\tau}$, the lower limit for the log law for the mean velocity should be Reynolds-number dependent rather than constant in wall variables. [See 2, 9].

TABLE I. Variation of the log-law constants for the mean velocity (κ and A) and variance (A_1 and B_1) with Re_τ . These are obtained from Eqs. (9) and (11) using log fits (Eqs. 7 and 10) in the range $1.2 \leq y/y_m \leq 13$.

Re_τ	κ	A	A_1	B_1
1,985	0.492	7.04	0.785	2.435
3,334	0.465	6.554	0.882	2.506
5,411	0.447	5.99	0.953	2.479
10,480	0.43	5.571	1.031	2.341
20,250	0.417	5.171	1.097	2.129
37,690	0.406	4.919	1.153	1.879
68,370	0.399	4.747	1.197	1.594
98,190	0.391	4.545	1.243	1.431

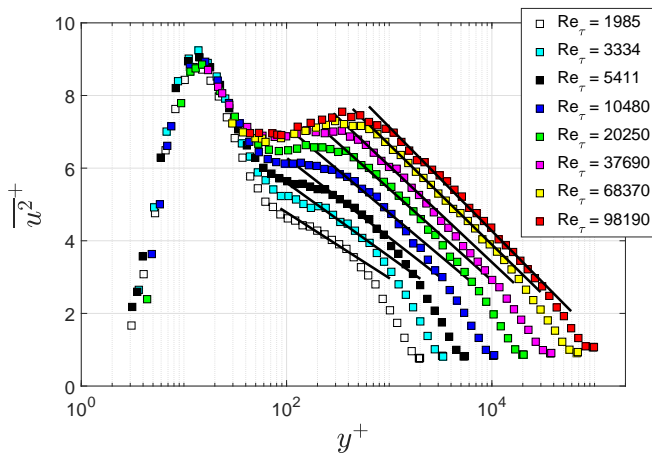


FIG. 4. Streamwise variance profiles for the pipe; solid lines are the classical log-law fits using A_1 and B_1 from table 1.

In Fig. 1, the Reynolds-number similarity of the streamwise variance for $y \approx y_m$ implies that, for $y > y_m$ there should exist a Reynolds-number-invariant log law scaled on the intermediate variables, and given as:

$$\frac{\overline{u^2}}{u_m^2} = B_1^m - A_1^m \ln\left(\frac{y}{y_m}\right). \quad (10)$$

To determine A_1^m and B_1^m , we fit a least-square straight line through the points in Fig. 1 (shown as a solid line) in the region $1.2 \leq y/y_m \leq 13$ for the two highest Reynolds numbers; this range is the same as that chosen for fitting a log law for the mean velocity in Overlap Layer II (Fig. 2). (The behaviour of $\overline{u^2}$ in Overlap Layer I is beyond the scope of the present work.) This gives $A_1^m = 0.178$ and $B_1^m = 1.005$. We do not attempt to estimate the uncertainty bounds for A_1^m and B_1^m (and also for κ_m and A_m ; Eq. 8) here, as their precise numerical values are not relevant for the key conclusions of the paper. The classical constants, A_1 and B_1 (Eq. 2), can be readily expressed in terms of A_1^m and B_1^m as

$$A_1 = A_1^m \left(\frac{u_m^2}{u_\tau^2}\right), \quad (11)$$

$$B_1 = \left[A_1^m \ln\left(\frac{y_m}{R}\right) + B_1^m\right] \left(\frac{u_m^2}{u_\tau^2}\right).$$

A_1 and B_1 calculated from Eq. (11) (with $A_1^m = 0.178$ and $B_1^m = 1.005$) are included in table 1; a clear trend in A_1 and B_1 with respect to Re_τ is evident. Fig. 4 shows the log-law fits to the variance, in wall variables, obtained by using A_1 and B_1 from table 1. As can be seen, the log fits inferred from Eq. (11) show a good match with the measured profiles in the intermediate region, over the entire Re_τ range. This leads us to conclude that the Townsend-Perry ‘constant’, A_1 , actually shows a systematic dependence on Re_τ even for $Re_\tau > 2 \times 10^4$. This is due to the fact that A_1^m and B_1^m

are Reynolds-number invariant and that u_m/u_τ (Fig. 3a) and $y_m/R (= 3.5/\sqrt{Re_\tau})$ show a continuous dependence on Re_τ . Furthermore, the values of A_1 in table 1 are entirely consistent, at corresponding Reynolds numbers, with those in Perry et al. [10] ($A_1 = 0.9$ for $Re_\tau \leq 3,900$) and Hultmark et al. [16] ($A_1 = 1.25$ for $Re_\tau = 98, 190$); Marusic et al. [2] reported $A_1 = 1.23 \pm 0.05$ for the same Re_τ), and provide an explanation for the observation.

We are grateful to Professor Lex Smits for use of the NSTAP data. We acknowledge financial support from EPSRC under Grant No. EP/I037938/1.

* sdiwan@iisc.ac.in; Present address: Department of Aerospace Engineering, Indian Institute of Science, Bangalore 560012.

† j.morrison@imperial.ac.uk

- [1] A. A. Townsend, *The Structure of Turbulent Shear Flow* (Cambridge University Press, 1976).
- [2] I. Marusic, J. P. Monty, M. Hultmark, and A. J. Smits, *J. Fluid Mech.* **716**, R3 (2013).
- [3] A. E. Perry and M. S. Chong, *J. Fluid Mech.* **119**, 173 (1982).
- [4] T. von Kármán, *Gott. Nachr.* **1**, 58 (1930).
- [5] C. B. Millikan, in *Proceedings of the 5th International Congress on Applied Mechanics*, edited by J. P. den Hartog and H. Peters (Wiley, London, UK, 1938) pp. 386–392.
- [6] I. Marusic, B. J. McKeon, P. A. Monkewitz, H. M. Nagib, A. J. Smits, and K. R. Sreenivasan, *Phy. Fluids* **22**, 065103 (2010).
- [7] M. Wosnik, L. Castillo, and W. K. George, *J. Fluid Mech.* **421**, 115 (2000).
- [8] H. M. Nagib and K. A. Chauhan, *Phy. Fluids* **20**, 101518 (2008).
- [9] S. C. C. Bailey, M. Vallikivi, M. Hultmark, and A. J. Smits, *J. Fluid Mech.* **749**, 79 (2014).
- [10] A. E. Perry, S. Henbest, and M. S. Chong, *J. Fluid Mech.* **165**, 163 (1986).
- [11] M. Hultmark, *J. Fluid Mech.* **707**, 575 (2012).
- [12] M. Hultmark, M. Vallikivi, S. C. C. Bailey, and A. J. Smits, *J. Fluid Mech.* **728**, 376 (2013).
- [13] G. I. Barenblatt, *J. Fluid Mech.* **248**, 513 (1993).
- [14] M. V. Zagarola and A. J. Smits, *J. Fluid Mech.* **373**, 33 (1998).
- [15] B. J. McKeon, J. Li, W. Jiang, J. F. Morrison, and A. J. Smits, *J. Fluid Mech.* **501**, 135 (2004).
- [16] M. Hultmark, M. Vallikivi, S. C. C. Bailey, and A. J. Smits, *Phys. Rev. Lett.* **108**, 094501 (2012).
- [17] K. R. Sreenivasan and A. Sahay, in *Self-Sustaining Mechanisms of Wall Turbulence*, edited by R. Panton (Comp. Mech. Publ., 1997) pp. 253–272.
- [18] T. Wei, P. Fife, J. Klewicki, and P. McMurtry, *J. Fluid Mech.* **522**, 303 (2005).
- [19] N. Afzal, *Ing.-Arch.* **52**, 355 (1982).
- [20] J. C. Klewicki, *J. Fluid Mech.* **718**, 596 (2013).
- [21] M. Vallikivi, B. Ganapathisubramani, and A. J. Smits, *J. Fluid Mech.* **771**, 303 (2015b).
- [22] J. F. Morrison, B. J. McKeon, W. Jiang, and A. J. Smits, *J. Fluid Mech.* **508**, 99 (2004).